JOURNAL OF CATALYSIS 113, 120–128 (1988)

# Effect of Consecutive and Alternative Oxidation and Reduction Treatments on the Interactions between Titania (Anatase and Rutile) and Copper

MARGARITA DEL ARCO,* ALFONSO CABALLERO,† PILAR MALET,† AND VICENTE RIVES*,[1]

*Departamento de Química Inorgánica, Universidad de Salamanca, Avda. del Campo Charro s/n, 37007-Salamanca, Spain, and †Departamento de Química Inorgánica, Instituto de Materiales (CSIC), Sevilla, Spain

Received June 29, 1987; revised March 9, 1988

Titania (anatase and rutile)-supported copper systems have been prepared by a conventional impregnation technique (2.5% Cu/Ti atomic ratio). The effect of consecutive oxidation/reduction/oxidation and reduction/oxidation treatments at 770 K on the final materials has been studied by X-ray diffraction, transmission electron microscopy, temperature-programmed reduction, and visible–ultraviolet (diffuse reflectance) spectroscopy, as well as assessment of the texture of the solids by nitrogen adsorption at 77 K. Clustered CuO, detected by XRD, is formed on anatase, together with dispersed $Cu^{2+}$ species, that are dominant on rutile. On this support, migration of copper species into the bulk of the support crystallites takes place, leading to unreactive copper species, and so, hydrogen consumption during reduction is lower in rutile-supported systems than the expected value to reduce all $Cu^{2+}$ species to the metallic state. 

## INTRODUCTION

Methanol synthesis catalysts are one of the main targets in today's catalysis research and copper-based catalysts have proved to be highly useful for these purposes; however, the nature of the catalytically active sites in these copper-containing systems is still a matter of controversy (*1, 2*), as are the parameters controlling the formation of the catalyst precursors and their decomposition to the final material. On the other hand, steam reforming of methanol ($CH_3OH + H_2O = 3\ H_2 + CO_2$) is a very interesting, thermodynamically favored reaction that proceeds with high selectivity and activity over copper-containing catalysts (*3–5*). Bearing in mind these two facts, it is not surprising that research to optimize copper catalysts has deserved much attention in recent years. These catalysts usually contain copper supported on a suitable oxide support (silica, alumina, etc.), but in recent years the so-called strong metal–support interactions (SMSI) effect (*6*) has introduced a very outstanding variable in the study of oxide-supported catalysts; although initially observed with noble metals when supported on semiconducting oxides, it has recently been claimed that this effect also results when metals such as copper are supported on titania (*7–10*); both electronic and geometric interactions between the support and the supported phase have been claimed to explain such SMSI.

This system, $Cu/TiO_2$ (as well as all others where titania is used as a support), gives rise to a very interesting problem, as it is well known that the surface chemistry of both crystallographic phases of titania (anatase and rutile) is very different, thus potentially allowing different interactions with the precursors and probably different

[1] To whom correspondence should be addressed.



0021-9517/88 $3.00

properties of the supported metal and the final catalyst.

In the present paper, titania (anatase and rutile)-supported copper systems have been prepared and characterized by different physicochemical techniques, including X-ray diffraction (XRD), Vis–UV/DR (diffuse reflectance) spectroscopy, texture measurements, transmission electron microscopy (TEM), and temperature-programmed reduction (TPR). The results obtained indicate that the nature of the support (anatase or rutile) controls the dispersion degree, as well as the reducibility of the cupric species, and probably migration of these species into the bulk of the support crystallites.

## EXPERIMENTAL METHODS

### *Preparation of the Samples*

Two titania supports kindly supplied by Tioxide (UK) have been used. Support R (Ref. NP85/10) had been obtained by the chloride process (*11*), dried at 393 K and calcined at 673 K; support A (Ref. NP85/12), obtained through the sulfate process (*11*), had been calcined 2 h at 993 K. Before incorporation of the copper species, both supports were further calcined in our laboratory overnight at 770 K to eliminate adsorbed organic contaminants. A known amount of titania was impregnated with an aqueous solution of $Cu(NO_3)_2 \cdot 3H_2O$ (Merck, p.a.) in amounts chosen to yield solids with a Cu/Ti atomic ratio of 2.5% (ca. 2% Cu, w/w). After having been stirred at room temperature for 60 min, the solvent was slowly evaporated at 330 K and the solid thus obtained was dried overnight at 380 K. The final material was manually ground in an agate mortar and was oxidized ($O_2$ from S.C.O., 99.95%) and/or reduced ($H_2$, S.C.O., 99.998%) at 770 K for 2 h in a dynamic system, using a gas flow of 50 $ml_{STP}\ min^{-1}$.

When naming the samples, the letter indicating the support is followed by an H (reduction) or an O (oxidation), to indicate the treatment given under the above-indicated conditions.

### *Apparatus*

Chemical analysis for copper was carried out by atomic absorption in an EL-240 Mark 2 instrument. X-ray diffraction diagrams were recorded in a Philips PW-1030 instrument, using Ni-filtered CuK$\alpha$ radiation ($\lambda$ = 154.05 pm) and standard recording conditions. Transmission electron microscopy studies were performed in a Siemens Elmiskop 102 apparatus. Nitrogen (S.C.O., 99.99%) adsorption isotherms (77 K) to determine the surface texture of the samples were measured in a conventional high-vacuum Pyrex system with grease-free stopcocks and joints and provided with a mercury vapor diffusion pump and a MKS pressure transducer to monitor pressure changes during adsorption; the system had previously been calibrated with helium (S.C.O., 99.995%). Analysis of the isotherms for surface area determination and porosity assessment was carried out with the assistance of a BASIC computer program (*12*) run in an Apple Macintosh. Electronic spectra (visible–ultraviolet/diffuse reflectance) were recorded in the range 900–200 nm in a Shimadzu UV-240 spectrophotometer provided with a diffuse reflectance accessory and a Shimadzu PR-1 graphic printer, using MgO or parent $TiO_2$ (anatase, A, or rutile, R) as the reference; the samples were kept in a specially built quartz cell that enables recording of the spectra under controlled atmosphere conditions. For temperature-programmed reduction studies, a mixture of $H_2$ and Ar (5%, 10 ml $min^{-1}$) from S.E.O. was used; the gas was previously passed through a $CO_2$/acetone trap to withdraw any condensable impurity; heating rate (10 K $min^{-1}$) was controlled with a Theall Eng. Co. TP-2000 instrument; a conductivity detector from Konik to determine hydrogen consumption was coupled to a Hewlett–Packard 3054-DL data station. Deconvolution and analysis of the TPR diagrams and elimination of

the baseline were performed with the assistance of a BASIC program, assuming Gaussian-type desorption profiles.

## RESULTS

### *Chemical Analysis*

Both in samples obtained from support A and in those obtained using support R the loading of copper was 1.94% (w/w), equivalent to a Cu/Ti atomic ratio of 2.5%.

### *X-Ray Diffraction*

As samples had to be exposed to air during manipulation to place them in the diffractometer to record the X-ray diffraction diagrams, and partial oxidation of the reduced samples on contact with air could not then be avoided, only X-ray diffraction diagrams of the supports and of all samples where the last treatment had been an oxidation have been recorded.

From maxima at 352 and 325 pm, corresponding to the most intense lines of anatase (100) and rutile (110) and using the equation proposed by Criado and Real (*13*), the weight percentages of anatase and rutile have been calculated for all these samples. In support R and in samples prepared on this support, the percentage of anatase was 3%, while in support A and samples prepared with it this percentage was 99%; the same crystallographic composition can then be safely assumed in the other samples. Incorporation of copper and further treatments in hydrogen and/or oxygen at 770 K does not modify these percentages within experimental error (±2%).

In copper-containing samples obtained with support R no maximum due to diffractions by Cu–O or Cu–Ti–O species could be observed; on the contrary, with samples obtained with anatase (support A) a very weak peak was recorded at 252 pm that can be ascribed to diffraction by (111) planes of CuO (*14*); nevertheless, the intensity of this peak is very low in these three samples (A–O, A–OHO, and A–HO).

### *Nitrogen Adsorption*

Nitrogen adsorption isotherms at 77 K on the supports and on samples indicated in Table 1 belong to type II according to IUPAC's classification (*15*), although in samples obtained using support A, a strong adsorption is observed for low relative pressures that suggests a partial character of type I isotherm. BET surface area values

TABLE 1

Preparation and Texture Properties of the Samples

| Sample | Support | Treatments at 770 K[a] | $S_{BET}$[b] | $S_{mp}$[b,c] |
|---|---|---|---|---|
| A | Anatase | Calcination | 9.4 | 1.9 |
| A–O | Anatase | O | 9.0 | 1.4 |
| A–OH | Anatase | O + H | n.m.[d] | n.m. |
| A–OHO | Anatase | O + H + O | 9.1 | 1.3 |
| A–H | Anatase | H | n.m. | n.m. |
| A–HO | Anatase | H + O | 9.6 | 0.5 |
| R | Rutile | Calcination | 15 | — |
| R–O | Rutile | O | 14 | — |
| R–OH | Rutile | O + H | n.m. | n.m. |
| R–OHO | Rutile | O + H + O | 12 | — |
| R–H | Rutile | H | n.m. | n.m. |
| R–HO | Rutile | H + O | 14 | — |

[a] O, oxidation; H, reduction.
[b] Square meters per gram.
[c] From the *t* method.
[d] n.m., not measured.

for samples obtained on support R were 13 ± 1 $m^2 g^{-1}$, slightly lower than the value calculated for the support calcined at 770 K, 15 $m^2 g^{-1}$. For support A, the BET specific surface area was 9.4 $m^2 g^{-1}$, and analysis of the isotherm following the *t* method developed by Lippens and de Boer (*16*) indicates the existence of micropores (i.e., pores with a diameter smaller than ca. 1.6 nm) which equivalent surface area amounts to 1.9 $m^2 g^{-1}$. For samples containing copper obtained with this support the specific surface area was 9.3 ± 0.3 $m^2 g^{-1}$, fairly close to that of the support; the surface area equivalent to adsorption in micropores was slightly lower than that determined for the calcined support.

*Transmission Electron Microscopy*

As for the X-ray diffraction and nitrogen adsorption studies, only samples where the last treatment had been an oxidation have been analyzed. No appreciable difference is observed among micrographs of samples prepared with a given support after copper loading, but differences are observed between both sets (on support A and on support R) of samples. Samples obtained on support R show a cylindric-capsule shape, but with a noticeably corrugated surface. On the contrary, samples obtained with support A display a pillbox-like shape with a smooth surface, at least as the magnification here used enables one to observe; in some of these particles, the formation of terraces is clearly seen. This different behavior of samples A and R has been previously observed by some of us (*12*) with titania samples similar to those used here as supports and calcined at 770 K, and so these differences are due to the support itself and not to the incorporation of copper.

*Visible–Ultraviolet Spectroscopy*

Spectra of all 10 samples, using the corresponding parent support as a reference, have been recorded. The precursors (i.e., after impregnation of the support with the copper nitrate solution and drying at 380 K) show slightly different colors: Precursor on support R is lighter (greenish-blue) and its vis–UV/DR spectrum shows a broad absorption band centered at ca. 780 nm; precursor on support A is sky blue and the broad band is centered around 830 nm. In both cases, the recorded band may be ascribed to the $^2E_g \rightarrow {}^2T_{2g}$ electronic transition of $Cu^{2+}$ species in an octahedral oxygen environment, distorted by a Jahn–Teller effect (*17*).

In the reduced state (R–OH, R–H, A–OH, A–H) all samples show a bluish-gray color that persists after exposure to air in the case of samples obtained using support R, but that slowly clears for samples obtained with support A, suggesting that an oxidation from $Cu^0$ to $Cu^{2+}$ takes place in these samples even at room temperature. After a prolonged exposure to air at room temperature, the color shown by these samples is identical to that of samples A–O and A–OHO. This fact suggests that copper, in the reduced state after reduction in hydrogen at 770 K, is more easily oxidized when supported on anatase than when supported on rutile.

Samples R–O, R–OHO, and R–HO show a yellowish color and their vis–UV/DR spectra are dominated by a band at 420 nm; in that of sample R–HO a very weak, broad band can be recorded at ≈770 nm, Fig. 1. For samples A–O, A–OHO, and A–HO, a continuous absorption is observed between 800 and 400 nm, and the samples show a light bluish-gray color. A very weak absorption at ≈720 nm is recorded for sample A–HO. That is, the absorption between 800 and 400 nm gives rise to the bluish-gray color, while only one band at 420 nm would account for the yellowish color in oxidized R samples. The origin of this band (that may be overlapped in the continuous absorption shown by oxidized A samples) has been previously ascribed (*18*) to the presence of surface peroxide species. Samples A–H and A–OH, exposed to air at room temperature for

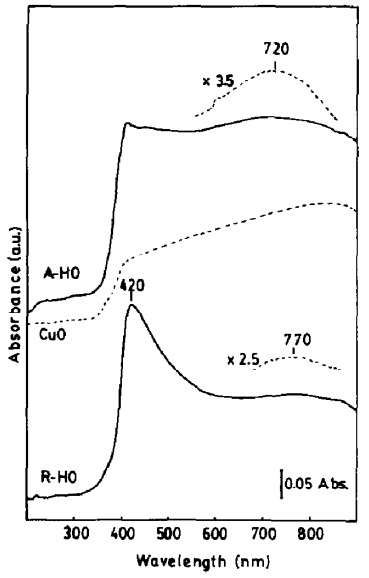


FIG. 1. Electronic spectra (diffuse reflectance) of samples A–HO and R–HO.

several days, display spectra that coincide with those of samples A–O and A–OHO, but a mere outgassing at room temperature recovers the original spectra.

Bands at 720 and 770 nm should be due to $Cu^{2+}$ species in a distorted octahedral oxygen coordination, and if their positions are compared with those of the bands displayed by the Vis–UV/DR spectra of the precursors, they are now recorded at lower wavelengths, indicating that the $Cu^{2+}$–O interaction has been enhanced after oxidation.

### *Temperature-Programmed Reduction*

TPR diagrams for all six oxidized samples containing copper are included in Fig. 2. In all cases, the baseline has been withdrawn and the spectra have been deconvolutioned, a minimum of four peaks being needed to achieve a good fit with the

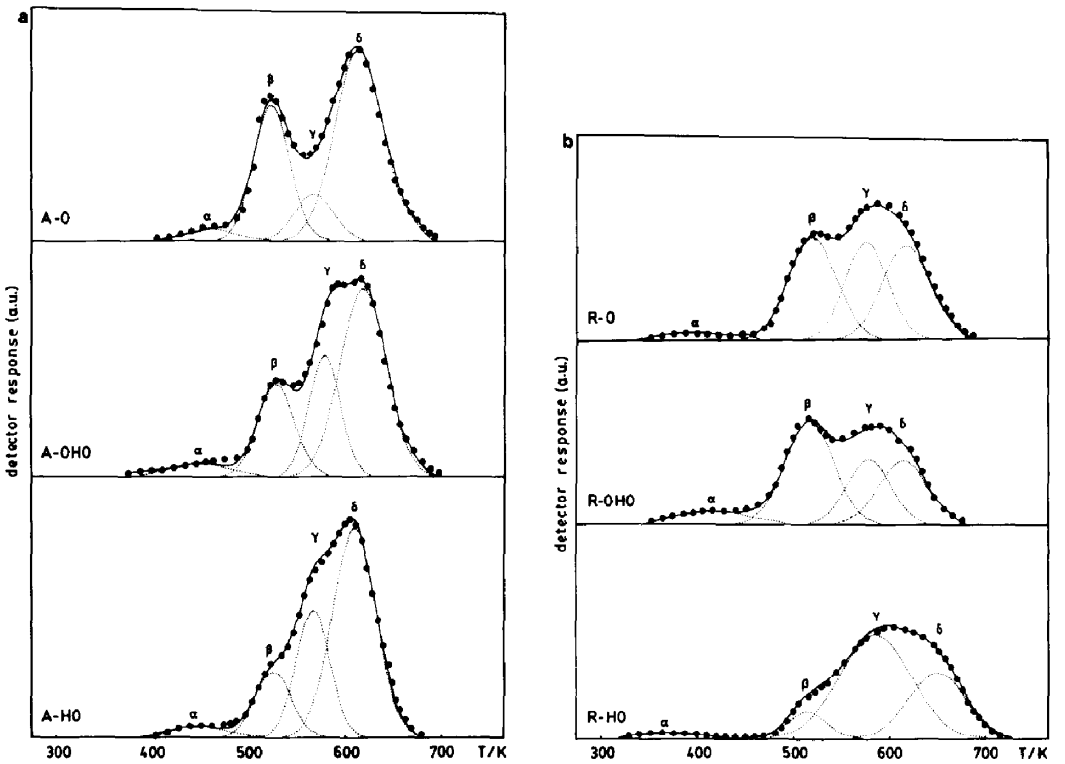


FIG. 2. (a) Programmed reduction profiles of samples A–O, A–OHO, and A–HO. (b) Programmed reduction profiles of samples R–O, R–OHO, and R–HO.

TABLE 2

Summary of TPR Data for the Oxidized Samples

| Sample | Total $H_2$ consumption[a] | mol $H_2$/mol Cu (temperature (K)) | | | |
|---|---|---|---|---|---|
| | | $\alpha$ | $\beta$ | $\gamma$ | $\delta$ |
| R–O | 269.6 | 0.03(391) | 0.29(517) | 0.25(573) | 0.31(614) |
| R–OHO | 206.6 | 0.05(414) | 0.29(514) | 0.15(576) | 0.19(611) |
| R–HO | 240.8 | 0.03(367) | 0.08(514) | 0.36(576) | 0.32(623) |
| A–O | 308.7 | 0.02(458) | 0.30(520) | 0.10(564) | 0.59(611) |
| A–OHO | 312.5 | 0.04(447) | 0.21(526) | 0.22(576) | 0.55(616) |
| A–HO | 314.6 | 0.03(444) | 0.14(523) | 0.25(564) | 0.61(607) |

[a] Micromoles $H_2$ per gram catalyst.

experimental TPR profile. Blank experiments with unsupported CuO have shown that reduction up to 770 K is enough to reduce all $Cu^{2+}$ species to the metallic state. A negligible amount of hydrogen was consumed during TPR of the unloaded supports.

Data on the amount of hydrogen consumed along the TPR runs in the temperature range 298–770 K, as well as the amounts corresponding to every one of the component bands, are included in Table 2. Taking into account the amount of copper existing in the samples, and assuming that in the oxidized samples all copper exists in the divalent state after oxidation at 770 K (by the way, thermodynamically favored), the amount of hydrogen required to complete reaction

$$CuO + H_2 \rightarrow Cu + H_2O$$

is 305.3 $\mu$mol $H_2$ (g cat.)$^{-1}$. As data in Table 2 show, this amount of hydrogen coincides, within experimental error, with that consumed along reduction of the oxidized samples obtained with support A. On the contrary, consumption of hydrogen during reduction of the oxidized samples obtained with support R is, in all cases, much lower than the expected value. Moreover, less hydrogen is consumed as the number of treatments given to the samples at 770 in $H_2$ *or* $O_2$ increases (R–O > R–HO > R–OHO), whichever the order and/or nature of these treatments.

## DISCUSSION

Data included above clearly indicate that both supports, rutile (R) and anatase (A), interact differently with copper under the experimental conditions used in this work.

Although in no case does heating in oxygen or in hydrogen at 770 K in the presence of copper favor the anatase → rutile phase change, it seems to be clear that on support R the copper is in a more dispersed state than on support A, as no peak due to diffraction by copper-containing species is recorded in the XRD diagrams of the former samples; this is not the case on samples A, XRD diagrams of which show a weak peak at 252 pm, ascribed to diffraction by (111) planes of CuO. The presence of this compound in samples A can be also inferred from the electronic spectra: the continuous absorption at 800–400 nm, responsible for the bluish-gray color of these samples after oxidation, is also recorded in the Vis–UV/DR spectrum of a mechanical mixture $CuO/TiO_2$–A, although in this case no absorption is recorded at 420 nm. That is, the spectra of samples obtained with support A seem to correspond to the continuous absorption due to the presence of CuO overlapped to the band at 420 nm, clearly recorded in the spectra of the R samples.

According to Kobayashi *et al.* (*19*), the copper loading modifies the final state of the catalyst; so, for low copper loading this

is highly dispersed on the support surface and no evidence of copper-containing species crystallites is found by XRD; however, if the metal loading increases, clustered CuO is formed, and similar conclusions have been reached from ESR results; the same effect has been observed by Delk and Vāvere (*7*). Nevertheless, this is not our case, as copper loading is the same in A- and R-supported samples as it is in the "low-content" level of Kobayashi and coworkers (*19*). So, the appearance of the peak due to CuO in the XRD diagrams of oxidized samples obtained on support A, and thus the formation of such undispersed supported phase, should be a result of a different interaction of copper with anatase (support A, formation of CuO crystallites) or with rutile (support R, no evidence of CuO crystallites). Moreover, XRD diagrams of Cu/R samples with the same Cu loading (in terms of surface coverage) as that for the Cu–A samples showed no peak due to CuO. This conclusion can also be reached from the Vis–UV/DR data above, as the continuous absorption between 800 and 400 nm is observed with A samples as well as with a mechanical mixture CuO/$TiO_2$.

Both supports had been calcined at 770 K before loading of copper. Prior to this treatment, support R had been calcined at 673 K, while support A had been calcined at 993 K. Then, successive treatments at 770 K in oxygen or in hydrogen may have had a larger effect on samples R than on samples A. According to the data in Table 1, there is a steady surface area decrease in samples R, from 15 $m^2\ g^{-1}$ (unloaded support R) to 12 $m^2\ g^{-1}$ (sample R–OHO), as the number of treatments at 770 K increases, while for samples obtained with support A the specific surface area remains nearly the same ($\pm 0.3\ m^2\ g^{-1}$). Unloaded support R submitted to these treatments shows no change in the specific surface area, and so the variation observed for series R samples can be related to the presence of well-dispersed (according to X-ray diffraction data) copper in these samples. On the contrary, support in samples A had already been stabilized by calcination at 993 K during manufacturing and so no change in its specific surface area is observed after further heatings at 770 K in the presence of copper, which on the other hand, is more poorly dispersed than in samples R.

According to the TE micrographs, mesoporosity in samples R should be related to the corrugated surface displayed by these cylinder capsule-shaped particles. The average geometric specific surface area that can be calculated for these particles from the micrograph, ignoring this corrugation, is ca. 10 $m^2\ g^{-1}$, noticeably lower than the value obtained by application of the BET method. For samples obtained with support A this calculation cannot be performed, as the pillbox-like shaped particles are oriented perpendicular to the observing direction and its width can hardly be estimated. However, formation of terraces in some of these particles is undoubtedly observed. Dimensions of micropores ($d < 1.6$ nm), the existence of which is concluded from application of the Lippens and de Boer method (*16*), make them unobservable, although they can be tentatively located near the break edges of the steps forming the terraces.

The different behavior of copper with anatase and rutile has already been pointed out very recently by Sermon *et al.* (*10*) from XPS and TPR measurements. These authors record two TPR peaks during reduction of CuO/$TiO_2$ systems that relate to the reduction of well and poorly dispersed $Cu^{2+}$ species, instead of to a-two step reduction $Cu^{2+} \rightarrow Cu^{+} \rightarrow Cu$, as the ESR spectrum is significantly unaffected before and after reduction at the point between both reduction peaks. On silica, Kobayashi *et al.* (*19*) have reported that reduction through the monovalent state takes place for low copper loading, but Delk and Vāvere (*7*) have reported one-peak TPR profiles in Cu/$SiO_2$ and discard this two-step process. If the presence of two TPR peaks would be due to

a stepwise reduction, the area of both peaks (i.e., the amount of consumed hydrogen) would be the same for both peaks, and this is not the case in Delk and Vāvere's (*7*) and Sermon *et al.*'s results (*10*).

In our samples, the situation seems to be rather more complicated and, as stated above, a good fitness between deconvolutioned and experimental TPR profiles is achieved only if *four* peaks are assumed, Table 2. Obviously, peak $\alpha$, amounting only for 0.02–0.05 mol $H_2$/mol Cu, can be an experimental artifact due to a miscancellation of the sloped baseline, but this is not the case for peaks $\beta$, $\gamma$, and $\delta$. Nevertheless, positions of these peaks are nearly the same in all six samples, indicating that they correspond to reduction of the same type of copper species, but existing in different amounts on the supports after the treatments given. In addition, the total consumption of hydrogen is much lower for samples R than the expected value, which coincides with that of samples A; this "lower-than-expected" consumption of hydrogen has also been observed by Sermon *et al.* (*10*) on rutile, but not on anatase, although these authors do not highlight this result. In our opinion, this can be explained following Sermon *et al.*'s conductivity results with anatase- and rutile-supported copper (*10*); according to these authors, the increased conductivity observed after reduction of the $Cu/TiO_2$–R system is due to the partial electron transfer $Cu^0 + Ti^{4+} \rightarrow Cu^{\delta+} + Ti^{3+}$ and simultaneous intercalation of copper to form bronzes, similarly to other well-known bronzes of vanadium or titanium. If this is the case in our samples, migration of copper species into the bulk of the rutile crystallites would partially inhibit its further oxidation and/or reduction, thus leading to a lower hydrogen consumption as the number of treatments in oxygen and/or hydrogen increases (see data in Table 2). Moreover, if this migration and reduction inhibition exists, the "oxidized" sample would still contain copper species in a nearly reduced state. Finally, reoxidation of the reduced A samples takes place even at room temperature, while for the R samples the reduced copper species existing in the bulk of the support crystallites are hardly oxidized at 770 K and not at all, of course, at room temperature. This migration may be assisted by the simultaneous sintering of the support crystallites that leads to a specific surface area decrease for R samples, but not for A samples. It should also be noted that the size of the octahedral holes in rutile is slightly larger than that in anatase (*20*), and so this migration would be easier in the former.

The relative intensities of the TPR peaks also change along the successive treatments; nevertheless, the position and intensity of peak $\delta$ for samples A remain unchanged (612 ± 5 K, 0.58 ± 0.03 mol $H_2$/mol Cu) and should correspond to reduction of the *same* amount of the *same* sort of $Cu^{2+}$ species; taking into account that XRD and Vis–UV/DR results above indicate the presence of CuO in these anatase samples, it can be tentatively concluded that peak $\delta$ in samples A is due to reduction of bulk CuO. In the case of samples obtained on support R, the lower intensity of peak $\delta$ in the TPR profiles would account for a lower content of CuO, thus being unobservable by XRD. Reduction of clustered CuO cannot account for the other TPR peaks instead of for peak $\delta$, as both peaks $\beta$ and $\gamma$ display lower areas in samples A than in samples R, and these CuO species have been detected by XRD and Vis–UV/DR in samples A.

With copper supported on silica, zirconia, and alumina, Kobayashi *et al.* (*19*) have also reported a shift and a variation in the number of TPR peaks as the copper content changes: with copper loadings similar to that used here (1.94%) two peaks are recorded, and for $Cu/SiO_2$ one of these peaks is at temperatures as high as 923 K. Although these authors relate the different behavior to the basicity of the support (basic metal oxides, like zirconia, would hold weakly the precursor species that then

would be more easily reduced), it should be noted that White *et al.* (*9*) find a different sort of interaction between copper and the oxide, according to the n- or p-type semiconducting properties of the support, giving rise to different electronic metal–support interactions. So, the conducting properties of the oxide, insulators (silica, alumina), n-type (titania) or p-type (zirconia) semiconductor, may account for the different strengths of the supported phase–support interaction and the ease of reduction; the different behavior observed in our work with rutile and anatase introduces a new variable in this study.

Assuming that our $\delta$ peak in the TPR profiles corresponds to reduction of bulk CuO (in other words, nondispersed cupric species), the question is still: Which is the origin of the remaining two peaks, $\beta$ and $\gamma$? It is tempting to ascribe them to a stepwise reduction of dispersed $Cu^{2+}$ to $Cu^0$, but in such a case both peaks would display identical areas, corresponding to consumption of the same amounts of hydrogen; this is not obviously the case, and the intensities of these two peaks in all six samples seem to follow a random change. They can be tentatively ascribed to well-dispersed copper species interacting in two different ways (with different strengths) with the support; in addition, in samples R another type of copper species should exist, which has migrated into the bulk of the support crystallites.

ACKNOWLEDGMENTS

The authors thank Professor M. Sánchez Camazano (CSIC, Salamanca), Dr. C. Otero (Universidad Complutense, Madrid), and Dr. F. Bea (Dpto. de Petrología, Salamanca) for their helpful assistance in obtaining some of the experimental results.

REFERENCES

1. Chinchen, G. C., and Waugh, K. C., *J. Catal.* **97,** 280 (1986).
2. Fleisch, T. H., and Mieville, R. L., *J. Catal.* **97,** 284 (1986).
3. Kobayashi, H., Takezawa, N., and Minochi, C., *Chem. Lett.*, 1347 (1976).
4. Minochi, C., Kobayashi, H., and Takezawa, N., *Chem. Lett.*, 705 (1979).
5. Kobayashi, H., Takezawa, N., and Minochi, C., *J. Catal.* **69,** 487 (1981).
6. Tauster, S. J., Fung, S. C., and Garten, R. L., *J. Amer. Chem. Soc.* **100,** 170 (1978).
7. Delk, F. S., II, and Vāvere, A., *J. Catal.* **85,** 380 (1984).
8. del Arco, M., and Rives, V., *React. Kinet. Catal. Lett.* **31,** 239 (1986).
9. Chen, H.-W., White, J. M., and Ekerdt, J. G., *J. Catal.* **99,** 293 (1986)
10. Sermon, P. A., Rollins, K., Reyes, P. N., Lawrence, S. A. Martin Luengo, M. A., and Davies, M. J., *J. Chem. Soc. Faraday Trans. I* **83,** 1347 (1987).
11. Darby, R. S., and Leighton, J., *in* "The Modern Inorganic Chemicals Industry" (R. Thompson, Ed.), p. 354. The Chemical Society, London, 1977.
12. Martin, C., Rives, V., and Malet, P., *Powder Technol.* **46,** 1 (1986).
13. Criado, J. M., and Real, C., *J. Chem. Soc. Faraday Trans. I* **79,** 2765 (1983).
14. Joint Committee on Powder Diffraction Standards, File No. 5-661 (1971).
15. Sing, K. S. W., Everett, D. H., Haul, R. A. W., Moscou, L., Pierotti, R. A., Rouquerol, J., and Siemieniewska T., *Pure Appl. Chem.* **57,** 603 (1985).
16. Lippens, B. C., and de Boer, J. H., *J. Catal.* **4,** 319 (1965).
17. Lever, A. B. P., "Inorganic Electronic Spectroscopy," 2nd ed., p. 554. Elsevier, New York, 1984.
18. del Arco, M., Holgado, M. J., Martín, C., and Rives, V., *Spectrosc. Lett.* **20,** 201 (1987).
19. Kobayashi, H., Takezawa, N., Shimokawabe, M., and Takahashi, K., *in* "Preparation of Catalysts" (G. Poncelet, P. Grange, and P. A. Jacobs, Eds.), Vol. 3, p. 697. Elsevier, Amsterdam, 1983.
20. Wells, A. F., "Structural Inorganic Chemistry," 4th ed. Oxford Univ. Press (Clarendon), Oxford, 1975.